

# Theoretical Analysis and Design of Dual Band DGS Antenna with Small Frequency Ratio for Wi-Fi and WiMAX Applications

Sachin Kumar<sup>1, \*</sup>, Alind P. Singh<sup>2</sup>, and Mukesh K. Khandelwal<sup>3</sup>

**Abstract**—In this article, a theoretical analysis and design are presented for a Microstrip Patch Antenna (MPA) embedded with an inclined rectangular slot supported by a C-shaped Defected Ground Structure (DGS). Dual-band characteristics are achieved at 2.4 GHz and 2.6 GHz with a small frequency ratio of 1.08, which makes the proposed antenna useable for Wi-Fi and WiMAX applications. A theoretical analysis is also proposed for the designed antenna structure using modal expansion cavity model and equivalent circuit approach. The analyzed antenna design is fabricated, and it is found that measured results are in good match with theoretical and simulated results.

## 1. INTRODUCTION

Microstrip Patch Antennas (MPAs) have been widely used due to their several design features such as low profile, light weight, simple fabrication and ease of integration with other planar circuits [1]. There have been several developments including multiband operations in MPAs within the last few years. Dual-band antennas have shown their better availability due to their extensive applications in the field of contemporary wireless communication. The dual-band design provides a wide range and combinations of frequency ratio, and these antenna designs have the flexibility to be tuned as per required application by simply changing the design parameters. By exciting  $TM_{10}$  and  $TM_{01}$  modes, the two frequencies can be generated; it can be achieved by using the single patch, multilayer stacked design or by dual-feed mechanism [2]. In a single-feed single-layer antenna, dual-band operation can be obtained by the technique of reactive loading, by cutting slots in the patch parallel to the radiating edge. This loading of slots makes the current flow longer in the patch, thus lowering the antenna fundamental frequency resulting in antenna size reduction. Various dual-band operating antennas have been designed and presented by several researchers across the globe, such as W-slot loaded rectangular patch [3], dual L-shape loaded patch [4], F-shaped shorted patch antenna [5], and two U-shaped slots loaded radiating microstrip patch [6]. Another technique for obtaining dual-band radiation is by stacking or by dual feeds. However, dual-feed antennas are not much preferred as they have complex feeding mechanism and are thus difficult to fabricate.

In the last few years, for dual-band applications, a number of stacked patch antennas have been proposed by several researchers. A stacked antenna with an H-shaped parasitic patch and U-shaped slot loaded fed patch [7], a stacked circular antenna with aperture coupled feeding [8], a coaxial feeding orthogonal slit cut circular patch stacked antenna [9], two elliptic patch with an air gap between them [10] are few among them. The main disadvantage of using multi-layered stacked patch antennas is their thick size. Because in the current communication scenario the focus is on miniaturized and thin components which can easily be integrated into small portable handheld devices. Thus, the use of stacking technique

---

*Received 21 September 2017, Accepted 10 November 2017, Scheduled 17 November 2017*

\* Corresponding author: Sachin Kumar (gupta.sachin0708@gmail.com).

<sup>1</sup> Department of Electronics & Communication Engineering, SRM University, Chennai, Tamil Nadu 603203, India. <sup>2</sup> Department of Electronics & Communication Engineering, Ajay Kumar Garg Engineering College, Ghaziabad, Uttar Pradesh 201009, India.

<sup>3</sup> Department of Electronics & Communication Engineering, Bhagwan Parshuram Institute of Technology, New Delhi 110089, India.

**Table 1.** Comparison of proposed antenna with other dual-band antennas.

Reference	Radiating bands	Frequency ratio
[3]	2.91 GHz 3.88 GHz	1.33
[4]	2.4 GHz 5 GHz	2.08
[5]	1.85 GHz 2.42 GHz	1.31
[6]	1.59 GHz 2.295 GHz	1.44
[7]	3.1 GHz 4.5 GHz	1.45
[8]	1.4 GHz 1.8 GHz	1.29
[9]	9 GHz 10.8 GHz	1.20
[10]	1.91 GHz 2.66 GHz	1.39
[11]	2.1 GHz 2.2 GHz	1.05
[12]	2.03 GHz 2.1 GHz	1.03
Proposed	2.4 GHz 2.6 GHz	1.08

is not very much efficient for the future handheld wireless equipment. The frequency ratio of the two bands is also an important parameter when designing the dual-band configuration. Most of the proposed antennas have a higher frequency ratio of the order around 1.5 or more than that [3–10]. A small number of proposed structures which have a small value of frequency ratio generally do not radiate for useful application bands [11, 12]. The frequency ratio comparison of the proposed antenna with other dual-band patch antennas is given in Table 1.

In this paper, an inclined slot loaded patch antenna with defected ground plane is proposed for dual-band operation. The phenomenon of varying the resonant frequency with the change in inclination angle of the slot has been utilized to tune the antenna for the frequencies of 2.4 GHz and 2.6 GHz. The antenna is easy to design and is fed by simple coaxial SMA connector feed. The theoretical analysis of the proposed antenna with Defected Ground Structure (DGS) is carried out using cavity model and circuit theory approach. The proposed antenna structure may be a good choice for a variety of wireless applications such as 2.4 GHz IEEE 802.11b, 802.11g and 802.11n standard based Wireless Local Area Network (WLAN), Bluetooth and public wireless hotspots applications. Another radiating band 2.6 GHz can be useful for Multichannel Multipoint Distribution Service (MMDS), IEEE 802.16 standard based Worldwide Interoperability for Microwave Access (WiMAX) and IEEE 802.20 based Mobile Broadband Wireless Access (MBWA).

## 2. ANTENNA DESIGN

The schematic of the proposed antenna is shown in Fig. 1. The proposed antenna consists of a rectangular patch of length  $L$  and width  $W$  fed with an SMA connector at a location of  $x_1$  and  $y_1$  as shown in the figure. An inclined rectangular slot of length  $l$  and width  $w$  with an inclination angle  $\psi$  is embedded on the patch. The ground plane of the proposed antenna is made defected by embedding a C-shaped ring slot which helps in achieving the desired dual-band frequency ratio. In Fig. 1(a), the top

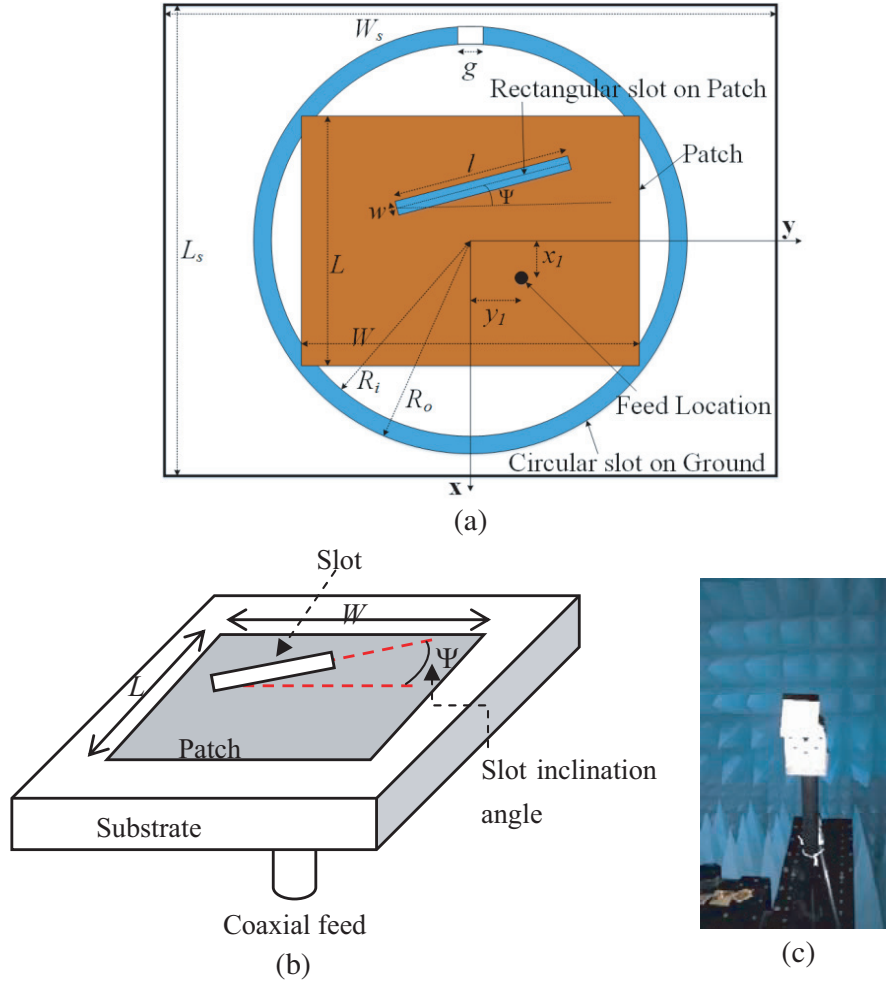


**Figure 1.** (a) Geometry of proposed inclined slot loaded patch antenna. (b) 3-D schematic showing radiating patch. (c) Fabricated prototype of proposed antenna during radiation pattern measurement in anechoic chamber.

and C-shaped defected ground bottom surface of the proposed antenna is shown while in Fig. 1(b) the 3-D schematic of inclined slot loaded patch is shown. Rogers RT Duroid-5880 with dielectric constant 2.2 and loss tangent 0.0009 of height 1.54 mm is used to design the proposed structure. The designed antenna is fed with coaxial feed by using a 50 ohm SMA connector. The dimensions of the proposed antenna are given in Table 2. A fabricated prototype of the proposed antenna is shown in Fig. 1(c). The antenna design simulations are done in FEM based available software tool HFSS.

### 3. THEORETICAL CONSIDERATIONS

The equivalent circuit of rectangular microstrip antenna is calculated as capacitance  $C_1$ , inductance  $L_1$  and resistance  $R_1$  connected in parallel [13]. Capacitance  $C_1$  can be calculated as

$$C_1 = \frac{\varepsilon_0 \varepsilon_e L^2}{2h} \cos^{-2} \left( \frac{\pi d}{L} \right) \quad (1)$$

where  $\varepsilon_e$  is the effective dielectric constant,  $d$  the feed point location  $(x_1, y_1)$ , and  $h$  the thickness of substrate. The effective dielectric constant can be evaluated as

$$\varepsilon_e = \frac{\varepsilon_r + 1}{2} + \frac{\varepsilon_r - 1}{2} \left( 1 + \frac{12h}{L} \right)^{1/2} \quad (2)$$

**Table 2.** Design details of inclined slot antenna with C-shaped defected ground plane.

Dimensions	unit(s)
Substrate Rogers RT/Duroid 5880 dielectric constant, $\varepsilon_r$	2.2
Thickness of the substrate, $h$	1.54 mm
Loss tangent of the substrate, $\tan \delta$	0.0009
Design frequency	3.0 GHz
Inclination angle, $\psi$	9 degree
Length of ground plane, $L_s$	55.6 mm
Width of ground plane, $W_s$	67.2 mm
Length of patch, $L$	32.7 mm
Width of patch, $W$	39.5 mm
Length of inclined slot, $l$	20 mm
Width of inclined slot, $w$	2 mm
External radius of C-shaped defect, $R_o$	25.8 mm
Internal radius of C-shaped defect, $R_i$	21.8 mm
Width of C-shaped defect ( $w_r = R_o - R_i$ )	4 mm
Width of strip connecting C-shaped defect, $g$	1.4 mm

$$L_1 = \frac{1}{\omega_r^2 C_1} \quad (3)$$

$$R_1 = \frac{Q_r}{\omega_r C_1} \quad (4)$$

$$Q_r = \frac{c\sqrt{\epsilon_e}}{4f_r h} \quad (5)$$

where  $\varepsilon_r$  is the relative dielectric constant of the substrate,  $f_r$  the resonance frequency of the patch, and  $c$  the velocity of light in free space

The rectangular patch input impedance is calculated as

$$Z_{patch} = \frac{1}{\frac{1}{R_1} + j\omega C_1 + \frac{1}{j\omega L_1}} \quad (6)$$

The impedance of the inclined slot using equivalent circuit approach comprises a resistance and a reactive component connected in series given by [14]

$$Z_{slot} = R_h + jX_h \quad (7)$$

where

$$R_h = 60\cos^2\psi [C + l_n(kl) - C_i(kl) + 0.5\sin(kl) \{S_i(2kl) - 2S_i(kl)\} + 0.5\cos(kl) \{C + l_n(0.5kl) + C_i(2kl) - 2C_i(kl)\}] \quad (8)$$

$l$  is the length of slot,  $\psi$  the inclination angle of slot from the radiating edge,  $C$  the Euler's constant, and  $k$  the propagation constant in free space defined as

$$k = \frac{2\pi}{\lambda} \quad (9)$$

$$S_i(x) = \int_0^x \frac{\sin x}{x} dx \quad (10)$$

$$C_i(x) = - \int_0^\infty \frac{\cos x}{x} dx \quad (11)$$

and

$$X_h = 30 \cos^2 \psi [2S_i(kl) + \cos(kl) \{2S_i(kl) - S_i(2kl) - \sin(kl) (2C_i(kl) - C_i(2kl) - C_i(kw^2/2l))\}] \quad (12)$$

where  $w$  is the width of slot.

The coupling capacitance used to couple the inclined slot with the patch is calculated as [15]

$$C_c = \frac{-(C_1 + C_s) + \left\{ (C_1 + C_s)^2 - 4C_1C_s(1 - C_k^{-2}) \right\}^{1/2}}{2} \quad (13)$$

where  $C_s$  is the slot capacitance, and  $C_k$  is given as

$$C_k = \left( \frac{L_1}{R_1 R_s C_s} \right)^{-1/2} \quad (14)$$

The impedance offered by coupling capacitance can be calculated as

$$Z_c = \frac{1}{j\omega C_c} \quad (15)$$

The equivalent circuit of inclined slot loaded rectangular patch antenna is shown in Fig. 2 and computed as

$$Z_{in} = Z_{slot} + \frac{1}{Z_c} + \frac{1}{Z_{patch}} \quad (16)$$

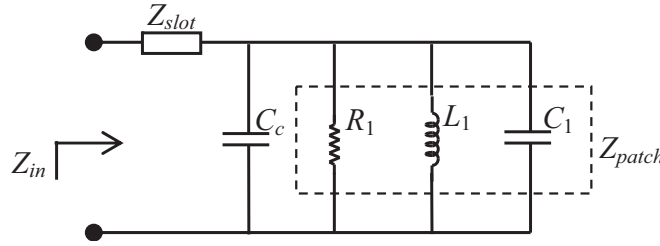


**Figure 2.** Equivalent circuit of rectangular patch.

The defected ground structures suppress spurious radiation and exhibit the properties similar to electromagnetic band gap (EBG) or wide stopband in performance. The C-shaped defected ground structure is used with the inclined slot loaded patch through an inductive coupling. The DGS with C-shaped design can be imagined as a lossy transmission line coupled to the transformer into the single line with electrical length. From  $ABCD$  matrix the complex propagation constant is derived as [16]

$$\gamma(f) = \alpha(f) + j\beta(f) \quad (17)$$

where  $\alpha(f)$  is the attenuation constant and  $\beta(f)$  the phase number. Since the equivalent parameters of the patch have been determined,  $Z_{patch}$  is the impedance of the patch antenna which is frequency dependent. The DGS can be viewed as a grounded transmission line with characteristic impedance of  $Z_g(f)$  and electrical length  $\theta_g \cong \lambda_g/2 \cong l_g$  [17]. Here, the coupling between the inclined slot loaded patch and C-shaped defected ground structure can be modeled by an ideal transformer, and the turn ratio  $n$  is calculated as [17]

$$n \cong \left( \frac{Z_{patch}(f)}{Z_g(f)} \right)^{1/2} \quad (18)$$

To determine the accurate circuit model shown in Fig. 3, firstly the input admittance  $Y_g$  of the defected ground structure is determined [16]

$$Y_g = \left[ Z_g(f) \cdot \frac{\tanh \alpha(f) l_g + j \tan \beta(f) l_g}{1 + j \tan \beta(f) l_g \tan \alpha(f) l_g} \right]^{-1} = Y_L \quad (19)$$

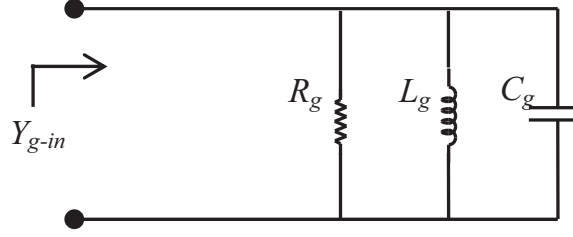


**Figure 3.** The equivalent circuit of the C-shaped circularly defected ground plane, with the elements  $R_g$ ,  $L_g$  and  $C_g$ .

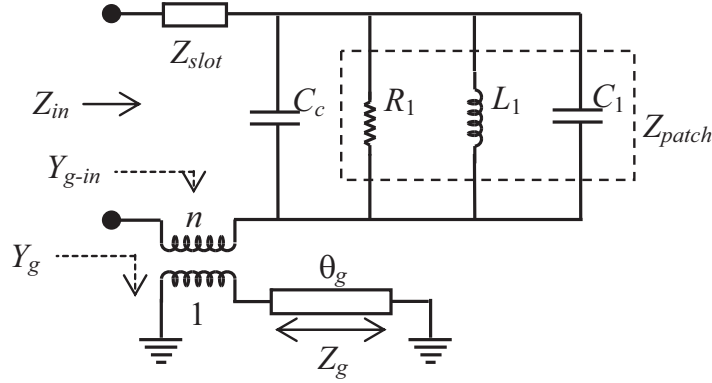


**Figure 4.** A circuit model for the C-shaped defected ground plane under an inclined slot loaded patch antenna.

Therefore, the equivalent circuit in terms of  $R_g$ ,  $L_g$ , and  $C_g$  can be determined as [18]

$$Y_{g-in} = \frac{Y_L}{n^2} = \frac{1}{R_g} + jB_g \quad (20)$$

where  $R_g = 1/\text{Re}[Y_{g-in}]$  represents the resistance in the parallel RLC tank circuit, corresponding with a lossy characteristic within the attenuation pole frequencies in the coupling of the patch and the defected ground plane. The inductance and capacitance can be found as

$$C_g = \frac{\text{Im}[Y_{g-in}]}{2\pi f_0 \left( \frac{f_0}{f_c} - \frac{f_c}{f_0} \right)} \quad (21)$$

$$L_g = \frac{1}{4\pi^2 f_0^2 C_g} \quad (22)$$

where  $f_c$  is the cutoff frequency of one-pole of the defected ground plane and  $f_0$  the attenuation pole frequency.

Figure 4 shows an equivalent circuit model of inclined slot loaded patch antenna etched on a C-shaped defected ground surface. The structure is printed on RT Duroid 5880 with design specifications as substrate thickness  $h$ , relative dielectric constant on the medium  $\epsilon_r$  and design frequency, provided in Table 2. The performance of the defected ground plane is as one-pole stopband filter, considering the parallel equivalent circuit model shown in Fig. 4. The reflection coefficient and VSWR can be calculated as [19]

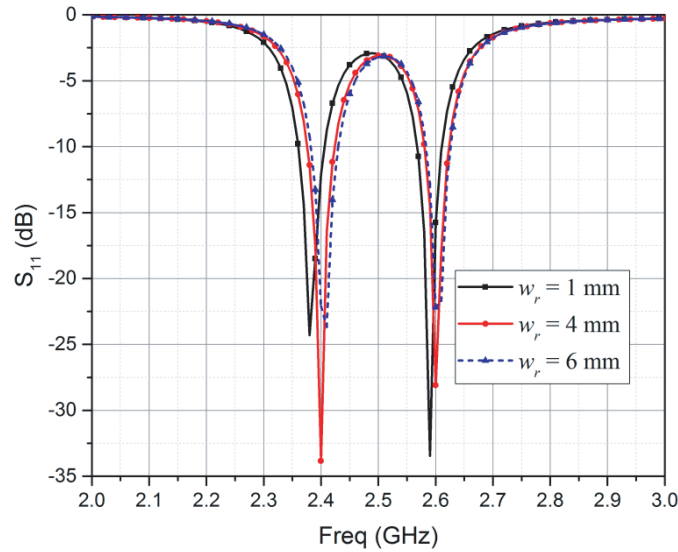
$$\Gamma = \frac{Z_o - Z_{eff}}{Z_o + Z_{eff}} \quad (23)$$

where  $Z_o$  is the characteristic impedance of the coaxial feed and  $Z_{eff}$  the total impedance calculated by considering C-shaped defected ground plane under an inclined slot loaded patch antenna

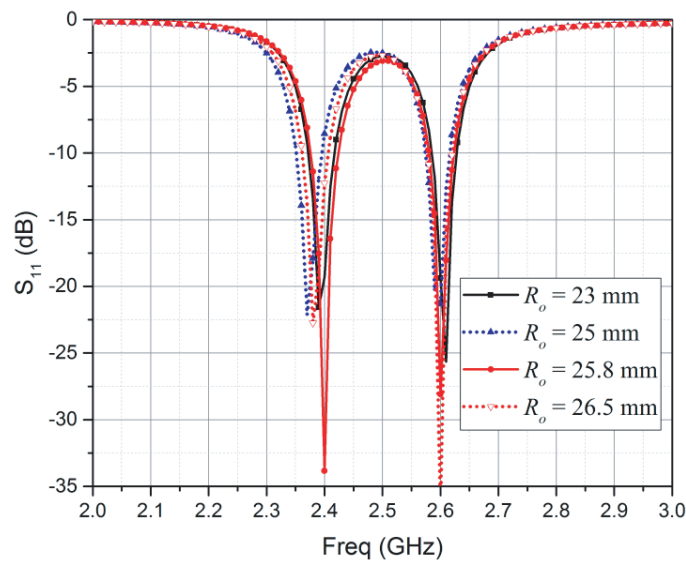
$$S = \frac{1 + |\Gamma|}{1 - |\Gamma|} \quad (24)$$

#### 4. RESULTS AND DISCUSSION

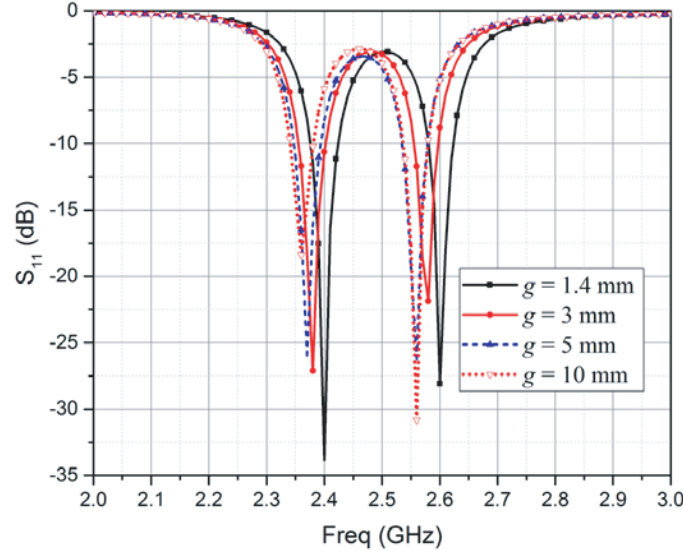
The parametric comparisons of the proposed dual-band structure for different antenna dimensions are illustrated from Fig. 5 to Fig. 10. Fig. 5 shows the return loss variation with frequency for different values of width  $w_r$  of C-shaped ring. The other parameters such as length and width of slot, angle of inclination, outer radius of C-shaped ring have been kept fixed during this variation. It can be observed from the graph that the antenna covers two application bands when the value of  $w_r$  is 4 mm. Fig. 6 illustrates the return loss variation for different values of outer radius  $R_o$  of C-shaped ring. In this comparison, the values of outer radius  $R_o$  and inner radius  $R_i$  of C-shaped ring are varied while keeping the width of ring fixed as 4 mm. It can be observed from the figure that at  $R_o = 28.5$  mm the antenna



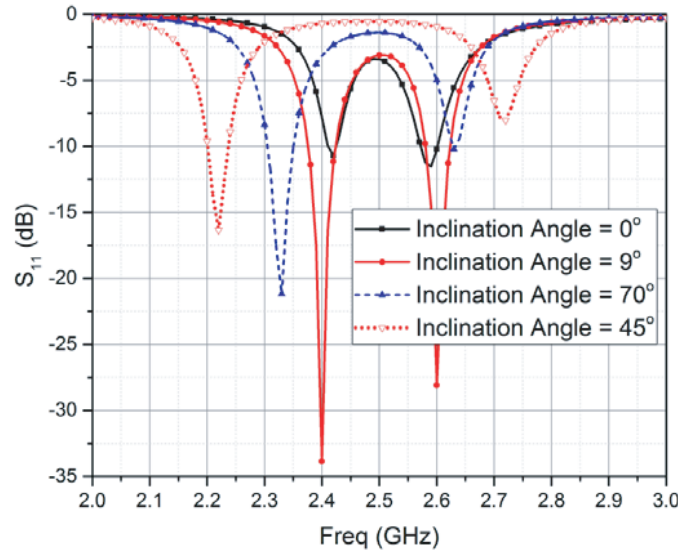
**Figure 5.** Variation in  $S_{11}$  with frequency for different values of width  $w_r$  of C-shaped ring for fixed outer radius  $R_o = 25.8$  mm.



**Figure 6.** Variation in  $S_{11}$  with frequency for different values of outer radius  $R_o$  of C-shaped ring for fixed width  $w_r = 4$  mm.



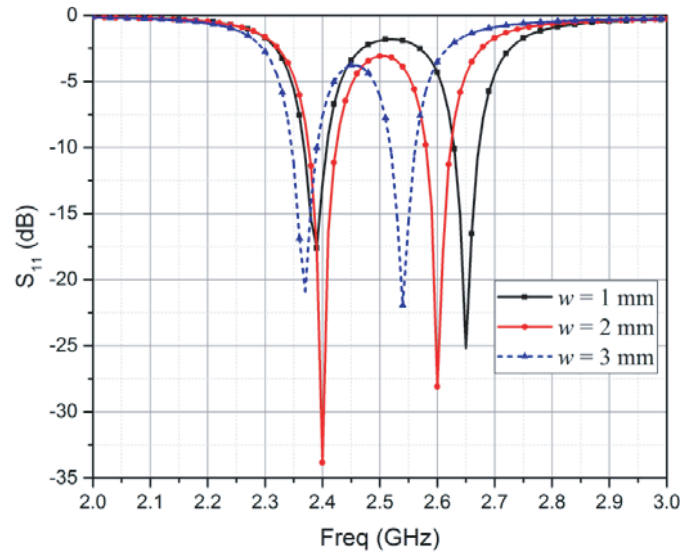
**Figure 7.** Variation in  $S_{11}$  with frequency for different values of gap  $g$  of C-shaped ring for fixed values of outer radius  $R_o = 25.8$  mm and width  $w_r = 4$  mm.



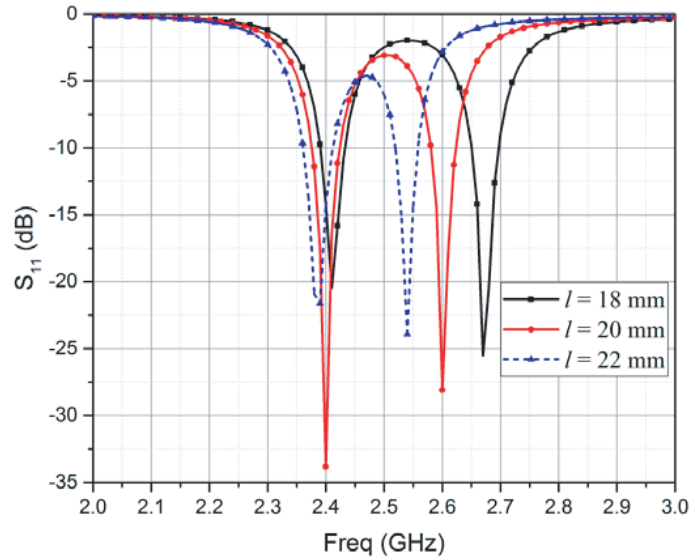
**Figure 8.** Variation in  $S_{11}$  with frequency for different values of angle  $\psi$  of rectangular slot with fixed values of outer radius  $R_o = 25.8$  mm and width  $w_r = 4$  mm.

radiates dual bands with center frequencies of 2.4 GHz and 2.6 GHz. The parametric comparison of  $S_{11}$  with frequency for different values of gap  $g$  of C-shaped ring is given in Fig. 7; for this variation, the values of outer radius  $R_o$  and width  $w_r$  are kept fixed as 25.8 mm and 4 mm, respectively. The best dual-band radiation is seen at width 1.4 mm, and it is also observed that for higher values of  $g$ , the dual bands shift towards lower frequencies. The return loss and frequency deviation for different angles  $\psi$  of rectangular slot is illustrated in Fig. 8. For inclination angle 70 degrees and 45 degrees, the antenna radiates only single band while at an angle of 0 degree the radiation is dual bands but with poor radiation characteristics. Here, it can be seen with an inclination angle of 9 degrees, the proposed antenna radiates dual bands with good radiation behaviour. Fig. 9 and Fig. 10 show the variation in return loss with frequency for different values of width  $w$  and length  $l$  of the inclined rectangular slot,





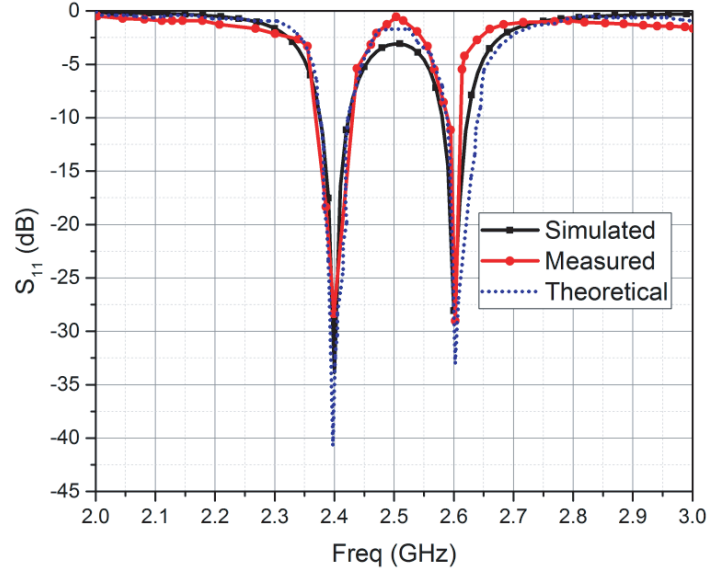
**Figure 9.** Variation in  $S_{11}$  with frequency for different values of width  $w$  of the rectangular slot with fixed values of outer radius  $R_o = 25.8$  mm and length  $l = 20$  mm.



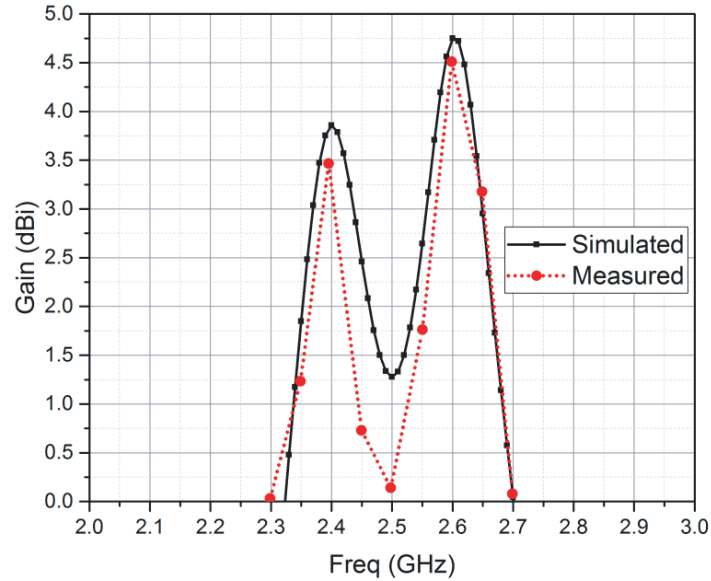
**Figure 10.** Variation in  $S_{11}$  with frequency for different values of length  $l$  of the rectangular slot with fixed values of outer radius  $R_o = 25.8$  mm and width  $w = 2$  mm.

respectively. The optimum dual-band radiation with better impedance matching is achieved at length 20 mm and width 2 mm. A shift in frequency bands is observed towards the lower side for greater values of width  $w$  and length  $l$  for the reason that larger values of length and width of loaded slot on the patch increase the current path present on the radiating patch thereby changing the resonance.

The proposed antenna structure is fabricated, and measurements are done using Agilent N5230 VNA. The return loss comparison of theoretical and simulated  $S_{11}$  with the measured result is shown in Fig. 11. It can be seen that all the three results match for the dual radiating bands. The first band radiates at a center frequency of 2.4 GHz and the second at 2.6 GHz. The design frequency of conventional rectangular dipole patch is 3 GHz; it is only after loading a rectangular slot of suitable dimensions in the patch a shift in radiating frequency band is observed. The dimensions of rectangular



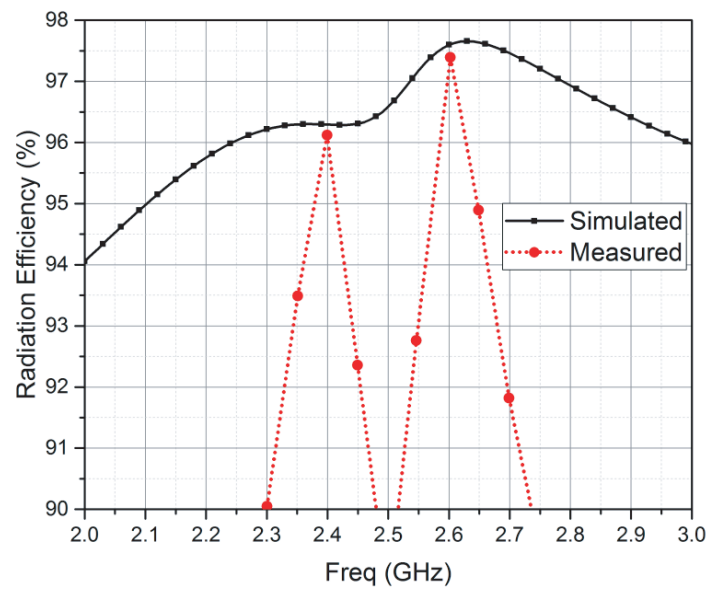
**Figure 11.**  $S_{11}$  variation with frequency of the inclined slot loaded defected ground antenna.



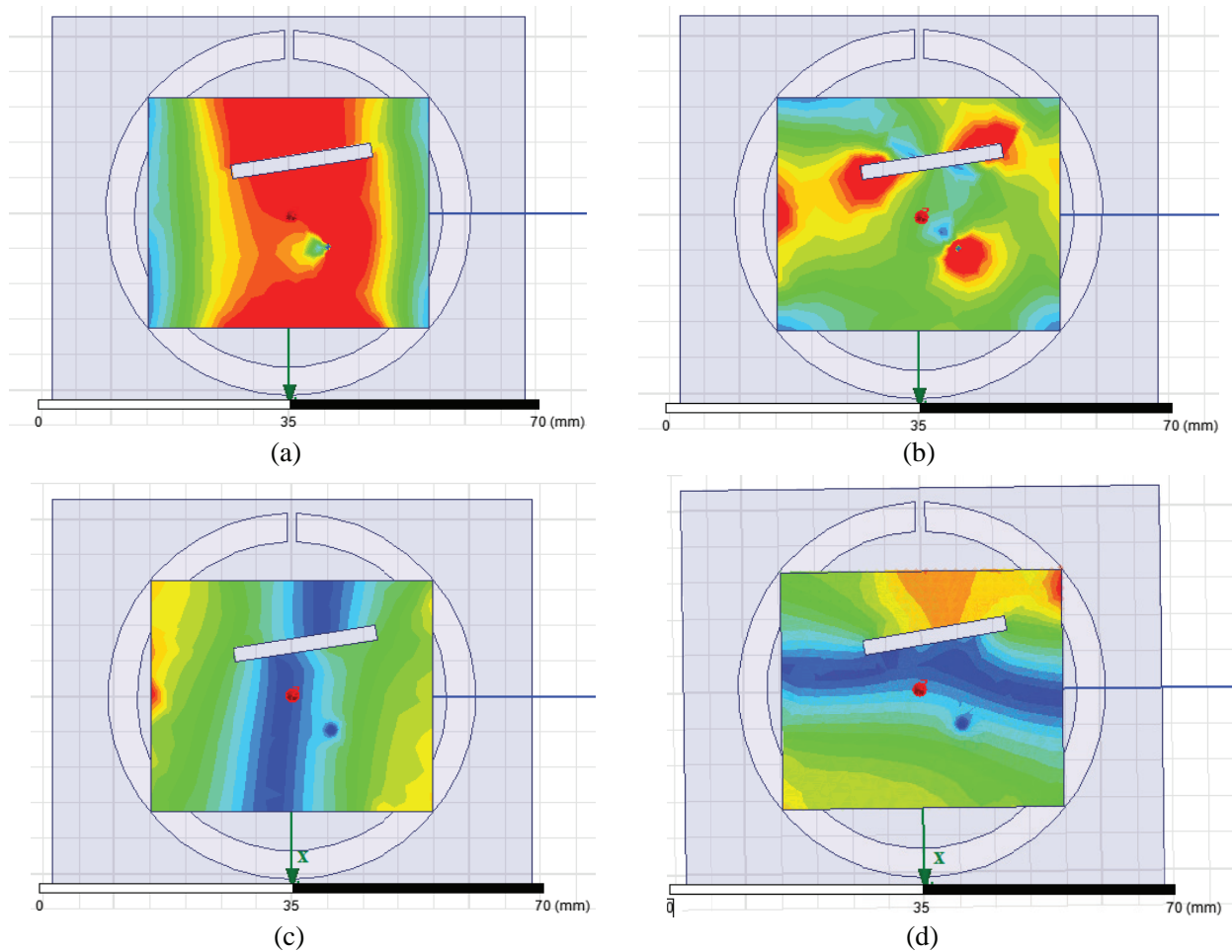
**Figure 12.** Gain variation with frequency of the inclined slot loaded defected ground antenna.

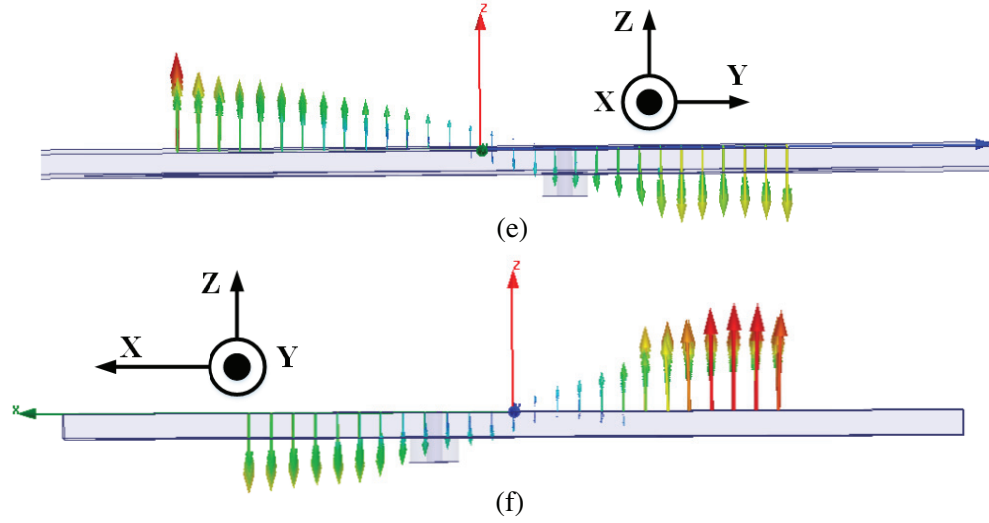
slot are optimized for achieving the application frequency band. By the effect of inductive or capacitive loading on the patch, a change in the current path on the radiating patch is observed; here the increased current path will shift the frequency to lower axis. The slotted patch antenna is advantageous in achieving compactness also because the antenna designed for higher frequency can be utilized for lower frequency bands subsequent to loading effects. The C-shaped ring slot embedded in the ground plane introduces a lower radiating band thus leading to two radiation bands. The frequency ratio of the two bands can be varied by varying the angle of inclined slot. By changing the radius of C-shaped ring, the lower radiating frequency can be altered. However, for the purpose of obtaining useful wireless application bands, here the optimized dimensions of C-shaped ring have been considered.

The gain variation of the proposed inclined slot loaded C-shaped defected ground antenna is shown



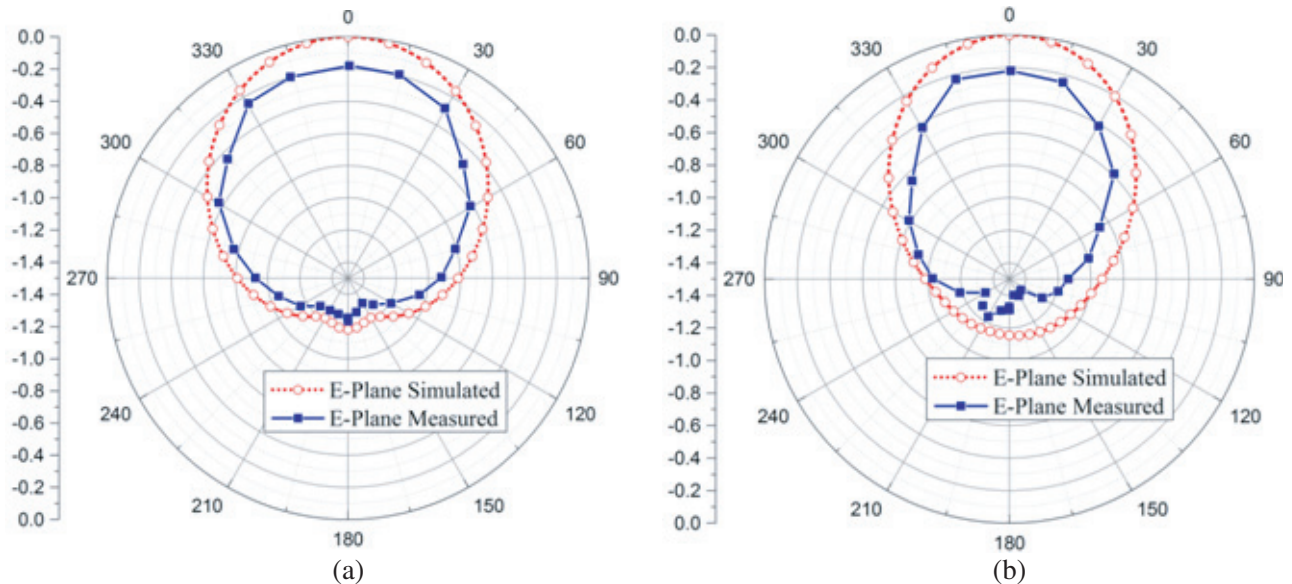
**Figure 13.** Radiation efficiency variation with frequency of the inclined slot loaded defected ground antenna.





**Figure 14.** Current and electric field distribution on the inclined slot loaded defected ground antenna. (a) Surface current density at 2.4 GHz. (b) Surface current density at 2.6 GHz. (c) Electric field distribution at 2.4 GHz. (d) Electric field distribution at 2.6 GHz. (e) TM<sub>01</sub> mode at 2.4 GHz. (f) TM<sub>10</sub> mode at 2.6 GHz.

in Fig. 12. The peak gain achieved at higher frequency band is more than 4.5 dBi. Fig. 13 illustrates the simulated and measured radiation efficiencies of the proposed antenna. The efficiency percentage is more than 90 percent for both the bands. A little variation in simulated and measured results is observed due to the connector soldering effects. The simulated current and electric field distribution are given in Fig. 14. The proposed antenna produces TM<sub>01</sub> mode at 2.4 GHz and TM<sub>10</sub> mode at 2.6 GHz as shown in Fig. 14(c), Fig. 14(e) and Fig. 14(d), Fig. 14(f), respectively. It can be observed that dual-frequency response differing by 8%  $\left[\frac{(2.6 - 2.4)}{((2.6 + 2.4)/2)} \times 100\right]$  is received due to dual-mode excitation as shown in Fig. 14(e) and Fig. 14(f). The simulated and measured *E*-plane and *H*-plane radiation patterns of the inclined slot loaded defected ground antenna in both the frequency bands are shown in Fig. 15. Fig. 16 shows the 3-D radiation pattern of the proposed inclined slot loaded defected ground antenna.



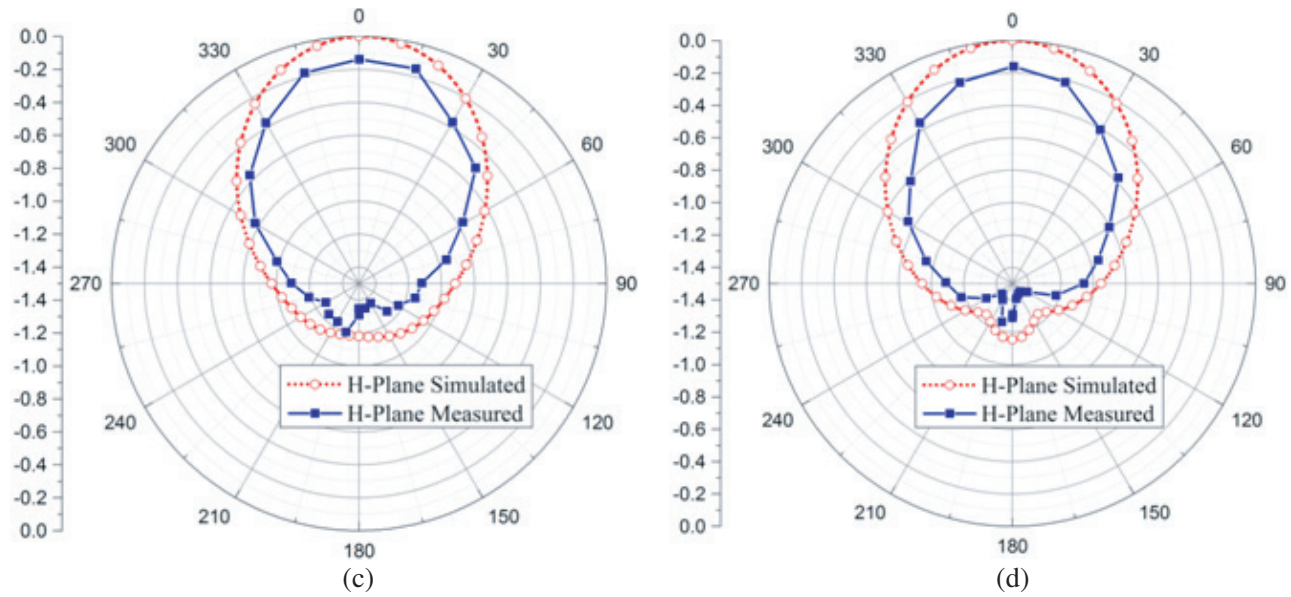


**Figure 15.** Radiation pattern of the inclined slot loaded defected ground antenna. (a) E-field at 2.4 GHz. (b) E-field at 2.6 GHz. (c) H-field at 2.4 GHz. (d) H-field at 2.6 GHz.

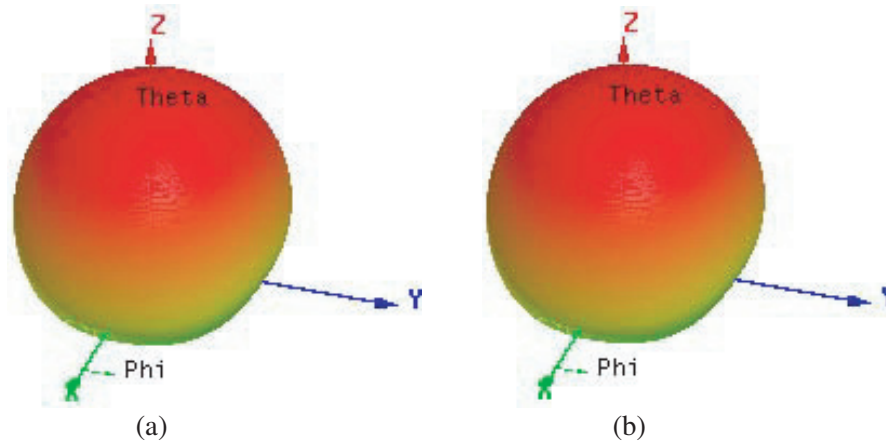


**Figure 16.** 3-D radiation pattern of the inclined slot loaded defected ground antenna. (a) 2.4 GHz. (b) 2.6 GHz.

## 5. CONCLUSION

In this paper, design and analysis of an inclined slot loaded patch antenna with C-shaped defected ground plane are successfully carried out. The simulated results are validated by theoretical and experimental results with the dual-frequency resonating at 2.4 GHz and 2.6 GHz. The proposed antenna has a small frequency ratio with both the usable frequency bands. The antenna has a simple coaxial feed and can be designed very easily. The proposed antenna structure may be a good candidate for 2.4 GHz IEEE 802.11 standard based WLAN and 2.6 GHz IEEE 802.16 standard based WiMAX applications.

## REFERENCES

1. Lo, Y. T., D. Solomon, and W. F. Richards, "Theory and experiment on microstrip antennas," *IEEE Trans. Antennas Propag.*, Vol. 27, 137–145, 1979.

2. Kumar, G. and K. P. Ray, *Broadband Microstrip Antennas*, Artech House, USA, 2003.
3. Ansari, J. A., A. Mishra, N. P. Yadav, P. Singh, and B. R. Vishvakarma, "Analysis of W-slot loaded patch antenna for dualband operation," *Int. J. Electron. Commun.*, Vol. 66, 32–38, 2012.
4. Wang, E., J. Zheng, and Y. Liu, "A novel dual-band patch antenna for WLAN communication," *Progress In Electromagnetics Research C*, Vol. 6, 93–102, 2009.
5. Kan, J. H. K. and W. S. T. Rowe, "Dual frequency F-shaped shorted patch antenna," *Microwave Opt. Technol. Lett.*, Vol. 48, 1811–1812, 2006.
6. Guo, Y.-X., K.-M. Luk, and K.-F. Lee, "A dual-band patch antenna with two U-shaped slots," *Microwave Opt. Technol. Lett.*, Vol. 26, 73–75, 2000.
7. Ansari, J. A., P. Singh, S. K. Dubey, R. U. Khan, and B. R. Vishvakarma, "H-shaped stacked patch antenna for dual band operation," *Progress In Electromagnetics Research B*, Vol. 5, 291–302, 2008.
8. Karmakar, N. C. and M. E. Bialkowski, "Circularly polarized aperture-coupled circular microstrip patch antennas for L-band applications," *IEEE Trans. Antennas Propag.*, Vol. 47, 933–940, 1999.
9. Gupta, S. K., A. Sharma, B. K. Kanaujia, S. Rudra, R. R. Mishra, and G. P. Pandey, "Orthogonal slit cut stacked circular patch microstrip antenna for multiband operations," *Microwave Opt. Technol. Lett.*, Vol. 55, 873–882, 2013.
10. Jan, J. Y. and K. L. Wong, "A dual-band circularly polarized stacked elliptic microstrip antenna," *Microwave Opt. Technol. Lett.*, Vol. 24, 354–357, 2000.
11. Kumar, S., B. K. Kanaujia, M. K. Khandelwal, and A. K. Gautam, "Stacked dual-band circularly polarized microstrip antenna with small frequency ratio," *Microwave Opt. Technol. Lett.*, Vol. 56, 1933–1937, 2014.
12. Kumar, S., B. K. Kanaujia, M. K. Khandelwal, and A. K. Gautam, "Single-feed circularly polarized stacked patch antenna with small-frequency ratio for dual-band wireless applications," *Int. J. Microw. Wireless Technol.*, Vol. 8, 1207–1213, 2016.
13. Garg, R., P. Bhartia, I. Bahl, and A. Ittipboon, *Microstrip Antenna Design Handbook*, Artech House, Norwood, MA, 2001.
14. Wolff, E. A., *Antenna Analysis*, Artech House, Dedham, MA, 1988.
15. Kanaujia, B. K., M. K. Khandelwal, S. Dwari, S. Kumar, and A. K. Gautam, "Analysis and design of compact high gain microstrip patch antenna with defected ground structure for wireless applications," *Wireless Per. Commun.*, Vol. 91, 661–678, 2016.
16. Gupta, K. C., R. Garg, I. Bahl, and P. Bhartia, *Microstrip Lines and Slotlines*, Artech House, Norwood, NJ, 1996.
17. Caloz, C., H. Okabe, T. Iwai, and T. Itoh, "A simple and accurate model for microstrip structures with slotted ground plane," *IEEE Microw. Wirel. Compon. Lett.*, Vol. 14, 133–135, 2004.
18. Pozar, D. M., *Microwave Engineering*, Wiley, Hoboken, NJ, 2005.
19. Derneryed, A. G. and A. G. Lind, "Extended analysis of rectangular microstrip antennas," *IEEE Trans. Antennas Propag.*, Vol. 27, 846–849, 1979.